

Far Infrared Reflection and Raman Spectra of Complex Perovskite-Type Compounds, $\text{Ba}(\text{Mn}_{1/3}\text{Ta}_{2(1-x)/3}\text{Nb}_{2x/3})\text{O}_3$

Kunio TOCHI, Tomiyasu OHGAKU, Nozomu TAKEUCHI and Shuichi EMURA*

(Faculty of Technology, Kanazawa University, 2-40-20, Kodatsuno, Kanazawa-shi 920)
 (* The Institute of Scientific and Industrial Research, Osaka University, 8-1, Mihogaoka, Ibaraki-shi, Osaka 567)

複合ペロブスカイト型化合物固溶体 $\text{Ba}(\text{Mn}_{1/3}\text{Ta}_{2(1-x)/3}\text{Nb}_{2x/3})\text{O}_3$ の赤外反射スペクトル及びラマンスペクトル

土地邦生・大角富康・竹内 望・江村修一*

(金沢大学工学部, 920 金沢市小立野 2-40-20)
 (* 大阪大学産業科学研究所, 567 茨木市美穂ヶ丘 8-1)

Infrared reflection and Raman spectra of the complex perovskite-type compounds, $\text{Ba}(\text{Mn}_{1/3}\text{Ta}_{2(1-x)/3}\text{Nb}_{2x/3})\text{O}_3$ have been measured at $x=0.0, 0.1, 0.3, 0.5, 0.7, 0.9$ and 1.0 . Two mode behavior was observed for both end-members and all the solid-solution in the vibration of BO_6 -type octahedrons, where B indicates Mn, Ta and Nb ions. The coexistence of TaO_6 and MnO_6 octahedrons in solid solutions, however, resulted in the one-mode behavior, instead of the two-mode one. That is, these two octahedrons represent one-mode behavior.

[Received May 29, 1989; Accepted June 23, 1989]

Key-words : Complex perovskite-type solid solution ceramics, Far infrared reflection spectra, Raman spectra, Two-mode behavior, One-mode

1. Introduction

In the previous report,¹⁾ we measured the infrared reflection and Raman spectra for two complex perovskite ceramic compounds, $\text{Ba}(\text{Mn}_{1/3}\text{Ta}_{2/3})\text{O}_3$ and $\text{Ba}(\text{Ni}_{1/3}\text{Ta}_{2/3})\text{O}_3$, and found that there are two-mode behaviors in the inner vibrations of the BO_6 -type octahedrons, where B indicates Mn, Ta, and Ni ions. In the present investigation we study further the effect of the replacement of Ta^{5+} ions in $\text{Ba}(\text{Mn}_{1/3}\text{Ta}_{2/3})\text{O}_3$ by Nb^{5+} ions partially or completely by making the solid-solutions.

2. Experimental procedure

2.1 Sample preparation

Samples were made from the starting materials of reagent-grade BaCO_3 , MnCO_3 , Ta_2O_5 and Nb_2O_5 . They were mixed in the mole ratio to form $\text{Ba}(\text{Mn}_{1/3}\text{Ta}_{2(1-x)/3}\text{Nb}_{2x/3})\text{O}_3$ for $x=0.0, 0.1, 0.3, 0.5, 0.7, 0.9$ and 1.0 . The mixtures were ball-milled in pure water. After dried, they were heated at 1100°C for 4 h, cooled to room temperature and ground in pure water for 48 h. After they were again dried, they were pressed at 1×10^8 Pa into disks 14 mm in diameter and 2 mm thick and heated at 1600°C for 2 h in air. The heating rate was 270°C/h . Finally they were cooled to room temperature within 24 h. Sample faces were

polished to a mirror state.

2.2 XRD analysis

XRD patterns were measured at room temperature. Figure 1 shows the intensity of the (100)* reflection line in the D_{3d} hexagonal structure²⁾ as a function of x -value. It is seen that the intensity decreases with the increasing x -value. This indicates that the hexagonal superstructure of the solid-solution is gradually lost with increasing x -value.

2.3 Infrared reflection spectra

IR reflection spectra were measured by using a Fourier Transform IR monochromator at room

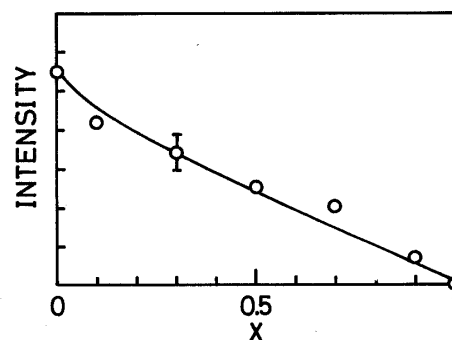


Fig. 1. Intensity of the (100)* reflection line for $\text{Ba}(\text{Mn}_{1/3}\text{Ta}_{2(1-x)/3}\text{Nb}_{2x/3})\text{O}_3$. This shows the formation of the D_{3d} hexagonal superstructure.

temperature. Figure 2 shows the result for the solid-solutions from $x=0.0$ to 1.0. All the reflection peaks were numbered from 1 to 6. Remarkable changes were hardly observed by changing the x -value, except that the peak numbered-6 grows with increasing x -value.

The reflection spectra were analyzed using the Kramers-Kronig relation.³⁾ TO-phonon frequencies were estimated from the positions of the maxima in the imaginary part, $\text{Im}(\epsilon)$, of the complex dielectric constant, $\epsilon = \epsilon' + i\epsilon''$, and LO-phonon frequencies were estimated from the maxima of $-\text{Im}(1/\epsilon)$, where Im indicates the imaginary part of the complex number. They are shown in Figs. 3(a) and 3(b) as functions of x -value.

The oscillator strengths of different modes are in proportion to the areas under the ϵ'' -curve. As an example, Fig. 4 shows the result of the Kramers-Kronig analysis for $x=1$, i. e., for $\text{Ba}(\text{Mn}_{1/3}\text{Nb}_{2/3})\text{O}_3$. It is seen from the figure, though the reflection peak numbered-6 and corresponding LO-peak are remarkable, that the related oscillator strength and the TO-phonon peak are very weak.

2.4 Raman spectra

Raman spectra were measured using an Ar laser at room temperature. As an example, Raman spectrum for $\text{Ba}(\text{Mn}_{1/3}\text{Ta}_{1/3}\text{Nb}_{1/3})\text{O}_3$ is shown in Fig. 5. Figure 6 shows the peak positions of the

spectra for all the solid solutions including the end-members. The results seem to be not very different from those in Fig. 2, especially there are similarities between the TO-mode peak positions and the Raman peak positions. However, the lines of peaks around 800, 420 and 380 cm^{-1} observed in Fig. 5 for Raman spectra are lost in the TO-modes as well as in the LO-modes in Fig. 2. It has been discussed that the 420 and 380 cm^{-1} Raman peaks are due to the torsional vibrations of the BO_6 -type octahedrons distorted into C_{4v} -symmetry.¹⁾ The F_{2u} -mode in the O_h -symmetry splits into the B_1 - and E -modes in the C_{4v} -symmetry, where the B_1 -mode vibration is forbidden in the IR reflection spectra, while both the B_1 - and E -modes are allowed in the Raman spectra. In addition, there is an experimental fact that the torsional E-mode is too weak to be detected in the reflection spectrum of a BaTiO_3 , whose symmetry is C_{4v} .⁴⁾ Therefore, the present absence of the torsional modes in the IR reflection spectra of the solid-solutions including the end-members, i. e., $\text{Ba}(\text{Mn}_{1/3}\text{Ta}_{2/3})\text{O}_3$ and $\text{Ba}(\text{Mn}_{1/3}\text{Nb}_{2/3})\text{O}_3$, can be understood that in these samples the BO_6 -octahedrons are distorted from

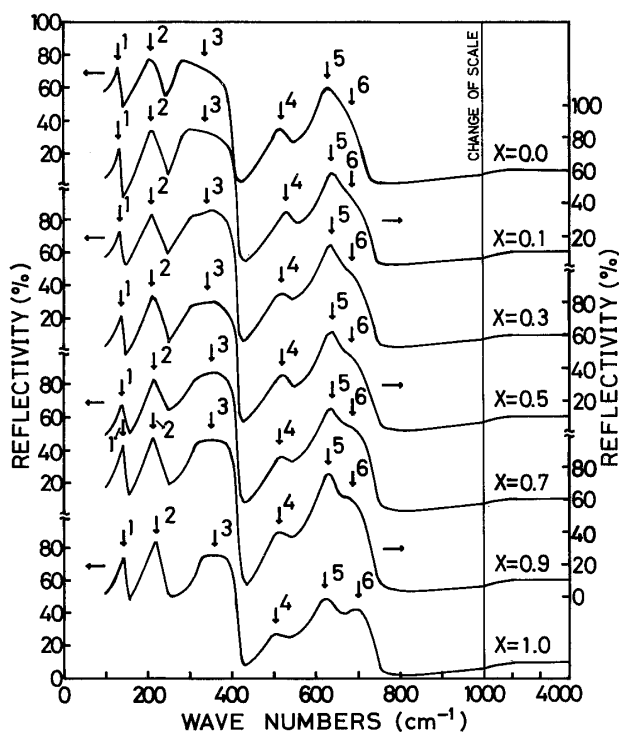


Fig. 2. Infrared reflection spectra for $\text{Ba}(\text{Mn}_{1/3}\text{Ta}_{2(1-x)/3}\text{Nb}_{2x/3})\text{O}_3$. Reflection bands are numbered from 1 to 6.

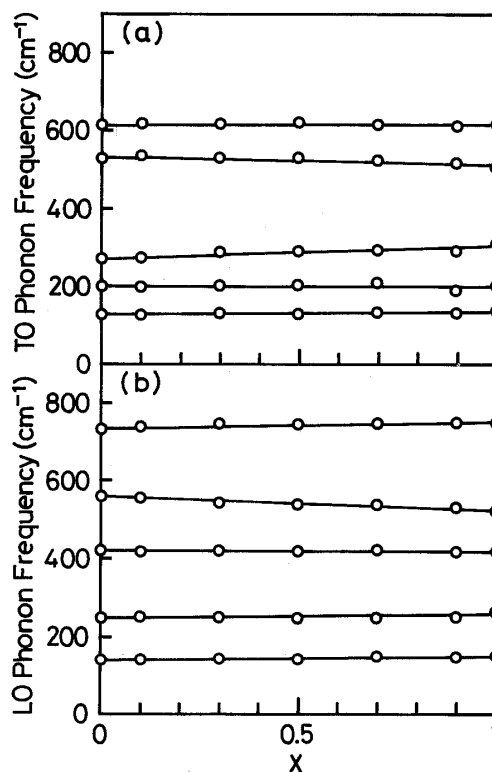


Fig. 3. Peaks for $\text{Im}(\epsilon)$ and $-\text{Im}(1/\epsilon)$ curves obtained by the Kramers-Kronig analysis of the reflection spectra, where $\epsilon = \epsilon' + i\epsilon''$ is the complex dielectric constant and Im indicates the imaginary part of the complex number. TO and LO phonon frequencies are shown by the peak frequencies of the $\text{Im}(\epsilon)$ and $-\text{Im}(1/\epsilon)$, respectively. They are shown in (a) and (b), respectively.

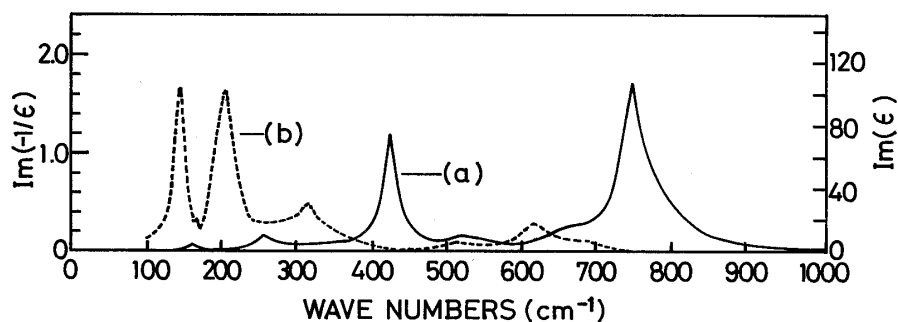


Fig. 4. An example of the Kramers-Kronig analysis for $x=1$, i. e., for $\text{Ba}(\text{Mn}_{1/3}\text{Nb}_{2/3})\text{O}_3$. Notice that $\text{Im}(\epsilon)$ is very weak around 700-800 cm^{-1} , while $-\text{Im}(1/\epsilon)$ is remarkable.

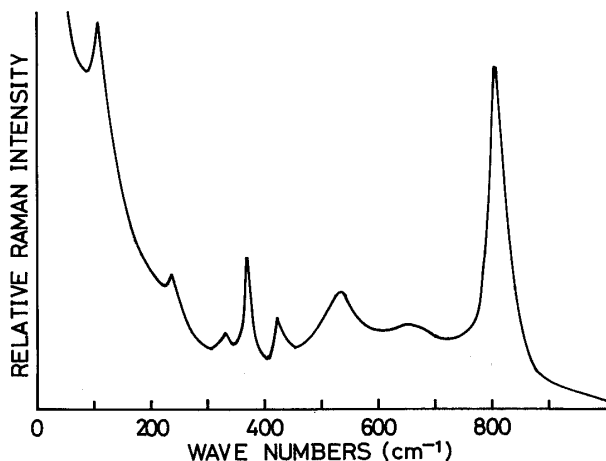


Fig. 5. An example of the Raman spectrum for $x=0.5$, i. e., for $\text{Ba}(\text{Mn}_{1/3}\text{Ta}_{1/3}\text{Nb}_{1/3})\text{O}_3$.

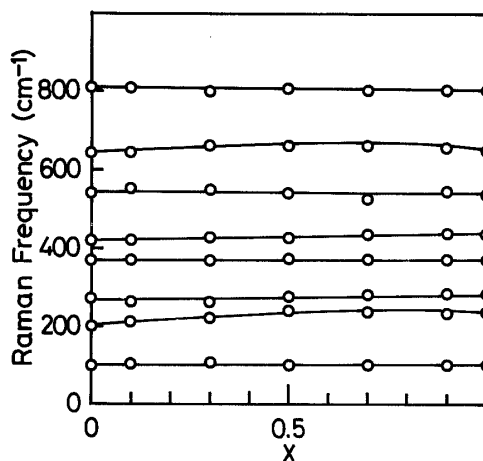


Fig. 6. Peak positions of the Raman spectra for $\text{Ba}(\text{Mn}_{1/3}\text{Ta}_{2(1-x)/3}\text{Nb}_{2x/3})\text{O}_3$.

O_h -symmetry, or at least they are not in the symmetry having a center of inversion.

3. Discussion

It has been reported by Perry and McCarthy,⁵⁾ that the IR reflection spectra for perovskite compounds such as CaTiO_3 , SrTiO_3 , BaTiO_3 , PbTiO_3 or their corresponding zirconates should show three reststrahlen bands related with the three triply degenerate infrared active modes. However, when the compounds are in cubic O_h -symmetry, the torsional modes of the BO_6 -octahedrons are not observed in both the IR and Raman spectra. When the octahedrons are distorted into, for instance, C_{4v} -symmetry, the torsional modes will be observed in the Raman,⁶⁾ and in some cases also in the IR reflection spectra.⁵⁾ Besides, there are cation- BO_3 lattice modes, which appear at the lowest frequencies of the spectra.⁵⁾ The spectra in Figs. 2 and 4, or the lines in Figs. 3 and 6 are in agreement with the above statement. This situation is again clearly understood from Table 1, in which the data for the endmembers are listed.

Table 1 shows that there are three groups of modes due to the inner vibrations of the BO_6 -octahedrons, in which each group splits further

into two modes: One is caused by the octahedron whose center is occupied by a Mn^{2+} ion, and the other is occupied by a Ta^{5+} or Nb^{5+} ion. It should be remarked that there are no splittings into two-mode behaviors due to the two octahedrons whose centers are occupied by Ta^{5+} and Nb^{5+} ions as has been directly seen from Figs. 3 and 6 for solid-solutions. Therefore, it can be said that the octahedrons related with the Ta^{5+} and Nb^{5+} ions show one-mode behaviors in their inner vibrations when they are in the solid-solutions.

This difference in the mode behaviors should have been caused by the difference in their valencies between Mn^{2+} and Ta^{5+} or Nb^{5+} ions. The difference in the atomic masses of these ions should be less important for the mode behaviors. The atomic mass for Mn, Nb, and Ta are 54.94, 92.91, and 180.95 amu, respectively. It is seen that the relative mass ratio of Mn to Nb is smaller than that of Nb to Ta. Therefore, if the difference in the atomic masses is more important than that in the valencies, two-mode behaviors of the Ta- and Nb-octahedrons should appear taking the precedence of those of Mn- and Ta- as well as Mn- and Nb-octahedrons.

We may further assume that in the solid-solution the disorder between Ta^{5+} and Nb^{5+} ions

Table 1. Infrared reflection and Raman data of $\text{Ba}(\text{Mn}_{1/3}\text{Ta}_{2/3})\text{O}_3$ and $\text{Ba}(\text{Mn}_{1/3}\text{Nb}_{2/3})\text{O}_3$ complex perovskite ceramics.

Modes	$\text{Ba}(\text{Mn}_{1/3}\text{Ta}_{2/3})\text{O}_3$			$\text{Ba}(\text{Mn}_{1/3}\text{Nb}_{2/3})\text{O}_3$		
	Infrared (cm^{-1})		Raman (cm^{-1})	Infrared (cm^{-1})		Raman (cm^{-1})
	(TO)	(LO)		(TO)	(LO)	
Unknown			806			801
Stretching Mode	620	736	640	620	749	661
	530	540	540	512	527	526
Torsional Mode	silent	silent	421	silent	silent	436
	silent	silent	370	silent	silent	373
Bending Mode	276	418	270	312	422	283
	198		200	198	259	235
(Cation- BO_3 Lattice Mode)	130	146		138	154	
Unknown			100			105

happens easier than the disorder between Mn^{2+} and those pentavalent ions, i. e., Ta^{5+} and Nb^{5+} ions, though the latter disorder may not completely be excluded.⁷⁾

On the other hand, the XRD intensity for the (100)* index shown in Fig. 1 is caused by the formation of superstructures resulting from the ordered configuration of these Mn^{2+} , Ta^{5+} , and/or Nb^{5+} ions. One would expect the compound with Ta^{5+} ions, as opposed to Nb^{5+} ions, to have more of a tendency to show a true homogeneous crystal on an atomic scale because of much larger mass difference between Mn and Ta than between Mn and Nb. We believe that the difference in the ionic radius between Ta^{5+} and Nb^{5+} is not so important, because the radii for Ta^{5+} and Nb^{5+} are 0.073 and 0.070 nm, respectively. Therefore, the monotonous decrease of the intensity of the (100)* line in Fig. 1 is in agreement with the above consideration of the mass difference that with increasing x -values, i. e., with increasing Nb^{5+} concentration, ordered configuration of the hexagonal superstructure disappears gradually.

It might be further considered that the disordering between the divalent Mn^{2+} and those pentavalent ions increases with increasing Nb^{5+} concentration, i. e., with increasing x -value because of the less difference in the mass ratio between Mn and Nb than Mn and Ta. The increase in the intensity of the reflection peak numbered-6 in Fig. 2 might be related with the suggestion of Barker and Sievers⁷⁾ that weak structure in a mixed crystal spectrum might be a normally inactive mode made active by the disorder.

References

- 1) K. Tochi, N. Takeuchi and S. Emura, *J. Am. Ceram. Soc.*, **72**, 158-60 (1989).
- 2) H. Tamura, T. Konoike, Y. Sakabe and K. Wakino, *J. Am. Ceram. Soc.*, **67**, C59-61 (1984).
- 3) F. Stern, "Solid State Physics Vol. 15", Ed. F. Seitz and D. Turnbull, Academic Press (1964) pp. 327-42.
- 4) W. Spitzer, R. C. Miller, D. A. Kleinmann and L. E. Wovarth, *Phys. Rev.*, **126**, 1710-21 (1962).
- 5) C. H. Perry and D. J. McCarthy, *Phys. Rev.*, **128**, A1537-38 (1965).
- 6) M. DiDomenico, Jr., S. H. Wemple and S. P. S. Porto, *Phys. Rev.*, **174**, 522-30 (1968).
- 7) A. S. Barker, Jr. and A. J. Sievers, *Rev. Mod. Phys.*, **47**, Suppl. No. 2, 1-179 (1975).